HHS Public Access

Author manuscript

Cell Rep. Author manuscript; available in PMC 2018 August 09.

Published in final edited form as:

Cell Rep. 2018 June 12; 23(11): 3340–3351.e5. doi:10.1016/j.celrep.2018.05.044.

Arabidopsis Duodecuple Mutant of PYL ABA Receptors Reveals PYL Repression of ABA-Independent SnRK2 Activity

Yang Zhao[1,7,*], **Zhengjing Zhang**[1,2,7], **Jinghui Gao**[3,4,7], **Pengcheng Wang**[1,3,7], **Tao Hu**[1,5,7], **Zegang Wang**[3], **Yueh-Ju Hou**[3], **Yizhen Wan**[3], **Wenshan Liu**[3], **Shaojun Xie**[3], **Tianjiao Lu**[1,2], **Liang Xue**[6], **Yajie Liu**[1,2], **Alberto P. Macho**[1], **W. Andy Tao**[6], **Ray A. Bressan**[3], and **Jian-Kang Zhu**[1,3,8,*]

[1]Shanghai Center for Plant Stress Biology, and CAS Center of Excellence in Molecular Plant Sciences, Chinese Academy of Sciences, Shanghai 200032, China

[2]University of Chinese Academy of Sciences, Beijing 100049, China

[3]Department of Horticulture and Landscape Architecture, Purdue University, West Lafayette, IN 47907, USA

[4]College of Animal Science and Technology, Northwest A&F University, Yangling, Shaan'xi 712100, China

[5]Key Laboratory of Plant Germplasm Enhancement and Specialty Agriculture, Wuhan Botanical Garden, Chinese Academy of Science, Wuhan 430074, Hubei, China

[6]Department of Biochemistry, Purdue University, West Lafayette, IN 47907, USA

SUMMARY

Abscisic acid (ABA) is an important phytohormone controlling responses to abiotic stresses and is sensed by proteins from the PYR/PYL/RCAR family. To explore the genetic contribution of PYLs toward ABA-dependent and ABA-independent processes, we generated and characterized high-order Arabidopsis mutants with mutations in the PYL family. We obtained a pyl quattuordecuple mutant and found that it was severely impaired in growth and failed to produce seeds. Thus, we carried out a detailed characterization of a pyl duodecuple mutant, pyr1pyl1/2/3/4/5/7/8/9/10/11/12. The duo-decuple mutant was extremely insensitive to ABA effects on seed germination, seedling growth, stomatal closure, leaf senescence, and gene expression. The activation of SnRK2 protein kinases by ABA was blocked in the duodecuple

[*]Correspondence: zhaoyang@sibs.ac.cn (Y.Z.), jkzhu@purdue.edu (J.-K.Z.).
[7]These authors contributed equally
[8]Lead Contact

AUTHOR CONTRIBUTIONS

J.-K.Z. and Y.Z. conceived and designed the research. Y.Z., Z.Z., J.G., P.W., T.H., Z.W., Y.-J.H., Y.W., W.L., T.L., Y.L., and L.X. performed the experiments. Y.Z., Z.Z., P.W., S.X., W.A.T., R.A.B., and J.-K.Z. analyzed the results. Y.Z., R.A.B., A.P.M., and J.-K.Z. wrote the manuscript.

DECLARATION OF INTERESTS

The authors declare no competing interests.

SUPPLEMENTAL INFORMATION

Supplemental Information includes three figures and three tables and can be found with this article online at https://doi.org/10.1016/j.celrep.2018.05.044.

mutant, but, unexpectedly, osmotic stress activation of SnRK2s was enhanced. Our results demonstrate an important role of basal ABA signaling in growth, senescence, and abscission and reveal that PYLs antagonize ABA-independent activation of SnRK2s by osmotic stress.

In Brief

Zhao et al. generated duodecuple and quattuordecuple Arabidopsis PYL ABA receptor mutants. Characterization of the mutants revealed that the ABA receptors are critical for plant growth and development and negatively regulate ABA-independent SnRK2 activity by interacting with and inhibiting osmotic stress-activated SnRK2 protein kinases.

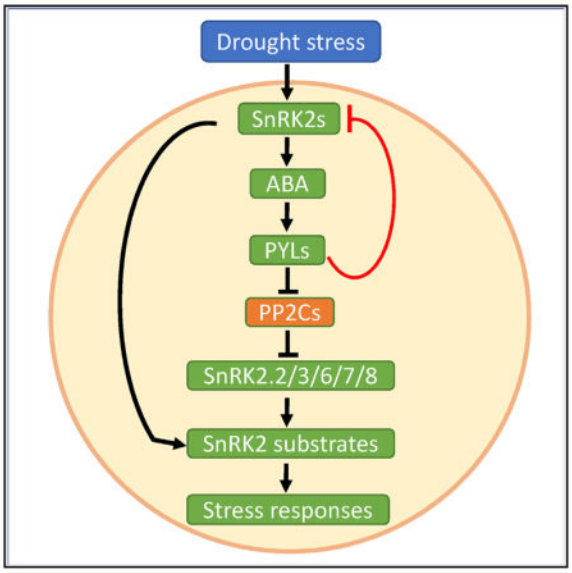

INTRODUCTION

The plant hormone abscisic acid (ABA) regulates plant growth, seed dormancy, leaf senescence, and responses to abiotic stresses (Cutler et al., 2010; Fujii and Zhu, 2009; Gonzalez-Guzman et al., 2012; Munemasa et al., 2015; Zhao et al., 2016). ABA is perceived by the intracellular pyrabactin resistance 1 (PYR1) and PYR1-like (PYL)/regulatory component of ABA receptor (RCAR) proteins (hereafter referred to as PYLs) (Ma et al., 2009; Park et al., 2009). All of the 14-members of PYLs, with the exception of PYL13, are able to respond to ABA and inhibit clade A PP2Cs in an ABA-dependent or -enhanced manner, resulting in the activation of sucrose non-fermenting 1-related protein kinase 2 s (SnRK2s) (Fujii et al., 2009; Fujii and Zhu, 2009; He et al., 2014; Li et al., 2013; Zhao et al., 2013). ABA-activated SnRK2s regulate the expression of ABA-responsive genes through phosphorylation of transcription factors, such as ABA-responsive element-binding factors (ABFs) (Furihata et al., 2006) and phosphorylate other substrates related to many processes. In unstressed plants, the target of Rapamycin (TOR) kinase phosphorylates PYLs to prevent activation of stress responses (Wang et al., 2018).

PYLs represent the largest family of hormone receptors in plants and function diversely and redundantly in ABA signaling (Ma et al., 2009; Park et al., 2009). PYLs selectively interact

with PP2Cs and selectively inhibit the phosphatase activity of the nine clade A PP2Cs (Antoni et al., 2012; Bhaskara et al., 2012; Tischer et al., 2017; Zhao et al., 2016). PYR1 and PYL1-2 are dimers in solution, while PYL4-6 and PYL8-10 are monomers (Dupeux et al., 2011; Hao et al., 2011). Generally, monomeric PYLs have higher binding affinities for ABA than dimeric PYLs in the absence of PP2Cs, and these monomeric PYLs can partially inhibit PP2Cs in the absence of ABA (Dupeux et al., 2011; Hao et al., 2011). PYL13 inhibits PP2CA in an ABA-independent manner but cannot inhibit ABI1, HAB1, and AHG1 even in the presence of ABA (Li et al., 2013; Tischer et al., 2017; Zhao et al., 2013). The diversity in these biochemical properties of PYLs is associated with natural variations of PYLs. Saturated mutations of PYR1 on residues that contact ABA or PP2Cs have been screened for the interaction of PYR1 and HAB1. Twenty-nine mutated PYR1 that have mutations located in 10 different residues (H60, V83, I84, L87, A89, M158, F159, T162, L166, and K170) interact with HAB1 without ABA (Mosquna et al., 2011). Among these mutations, V83L and I84K double mutations enable PYL2 to be a monomeric PYL with partially ABA-independent activity (Hao et al., 2011). Natural variations of H60P and I84K can be found in PYL7-9; three variations including H60P, V83L, and I84K can be found in PYL10; L166F can be found in PYL11; and moreover, four variations including H60R, V83L, L87F, and L166Y can be found in PYL13. The overlap of these mutations with natural variations partially explains the higher basic activities of monomeric PYLs and PYL13 in the absence of ABA and also explains the oligomeric status of these PYLs.

Based on the diversity of their expression patterns and biochemical properties, PYLs are expected to have functional diversity. The *pyr1* single mutant is resistant to pyrabactin, which led to the identification of PYL ABA receptors (Park et al., 2009). The *pyl8* single mutants are less sensitive to ABA-induced growth inhibition of primary roots compared with the wild-type (WT), whereas ABA-induced inhibition of lateral root elongation is enhanced in *pyl8* mutants (Antoni et al., 2013; Zhao et al., 2014). PYL8 promotes auxin responses by directly interacting with and enhancing the activities of MYB77 and its paralogs (Zhao et al., 2014). The *pyl9* single mutant shows a reduced ABA-induced leaf senescence under low light (Zhao et al., 2016). PYL9 promotes ABA-induced leaf senescence by activating ABFs through core ABA signaling in an ethylene-independent manner (Zhao et al., 2016). AtPYL13 and its rice ortholog OsPYL12 inhibit the phosphatase activity of some PP2Cs in the absence of ABA, and OsPYL12 is unable to bind to ABA (He et al., 2014; Li et al., 2013).

Osmotic stress inhibits plant growth and affects development. In response to osmotic stress, plants accumulate ABA, which subsequently induces ABA-dependent responses. Osmotic stress also activates ABA-independent responses through SnRK2s (Fujii et al., 2011). In *Arabidopsis*, the ten members of the SnRK2 family function redundantly in osmotic stress responses (Boudsocq et al., 2004; Fujii et al., 2011). Five SnRK2s including SnRK2.2, −2.3, −2.6, −2.7, and −2.8 are activated by ABA (Furihata et al., 2006). Understanding how PYLs affect ABA-dependent responses and ABA-independent osmotic stress responses requires genetic impairment of PYLs to block ABA signaling. The *pyr1 pyl1 pyl2 pyl4 pyl5 pyl8* T-DNA sextuple mutant (abbreviated as *112458*) and the CRISPR/Cas9-generated *pyl* sextuple mutant (abbreviated as *112458-C*) show strong ABA insensitivity in seed germination and seedling establishment, plant growth, stomatal movement, and expression of specific genes

(Gonzalez-Guzman et al., 2012; Zhang et al., 2016). Since the mutation in *PYL8* is in the 5′ untranslated region, the root length and fresh weight of *112458-C* mutant are lower than that of the *112458* T-DNA sextuple mutant under high concentration of ABA (Zhang et al., 2016). The *112458* mutant is also impaired in vegetative and reproductive growth (Gonzalez-Guzman et al., 2012), supporting that ABA signaling is required for plant growth and development. However, the growth of *112458* is still more robust than *snrk2.2/3/6*, and stomatal aperture of *112458* is smaller than that of *snrk2.2/3/6* (Gonzalez-Guzman et al., 2012). This suggests that other PYLs are still capable of activating some ABA signaling. Indeed, a *pyl9* single mutant shows reduced ABA-induced leaf yellowing under low light (Zhao et al., 2016). In this study, we generated a *pyl* quattuordecuple mutant and a *pyr1pyl1/2/3/4/5/7/8/9/10/11/12* (abbreviated as *112458 379101112*) duodecuple mutant using a CRISPR/Cas9 gene editing system. Our characterization of these high-order phytohormone receptor mutants provides important insights into the physiological function of PYLs in not only ABA-dependent plant processes but also ABA-independent osmotic stress responses.

RESULTS

Generation of pyl Duodecuple and Quattuordecuple Mutants

Using a multiplex CRISPR/Cas9 system described previously (Zhang et al., 2016), we generated two CRISPR/Cas9 constructs containing eight single guide RNAs (sgRNAs) and co-transformed these two constructs into the *112458 pyl* T-DNA sextuple mutant (Figures 1A and S1A; Table S1). One of these two constructs contained six sgRNAs, targeting six *PYLs* (*PYL3*, *PYL6*, *PYL7*, *PYL9*, *PYL11*, and *PYL12*), and the other construct contained two sgRNAs, targeting *PYL10* and *PYL13*. We were able to mutate six of these eight PYLs, generating the *112458 379101112 pyl* duodecuple mutant (Figure 1A). We then generated a *pyl6 pyl13* mutant in the *112458* background using CRISPR/Cas9 and crossed it with the *112458 379101112* mutant. We screened thousands of F2 seedlings and identified *pyl* quattuordecuple mutant plants with all 14 *PYLs* mutated (Figures 1B and 1C). In the *pyl* quattuordecuple mutants, PYL3-179insA resulted in a frameshift at codon 60; PYL6-140insT resulted in a frameshift at codon 47; PYL7-93insA resulted in a nonsense mutation at codon 30; PYL9-60insC resulted in a frameshift at codon 21; PYL10-Del225-263 resulted in a deletion from codon 75 to 87, which falls into the switch loop region for PP2C binding (Yin et al., 2009); PYL11-73insT resulted in a frameshift at codon 25; PYL12-Del67-71 resulted in a frame-shift at codon 23; and PYL13-Del391-394 resulted in a frameshift at codon 131 (Figures 1C and S1B). The *pyl* quattuordecuple mutant plants were severely impaired in growth in soil (Figure 1B). Although the *pyl* quattuordecuple mutants produced a few seeds on occasions, these seeds were all heterozygous, likely due to pollen pollution from adjacent plants, suggesting that the mutants were male sterile. Thus, we were only able to carry out further analysis on the *112458 379101112* mutant.

We also transformed the construct containing the six sgRNAs into Col-0 and generated the *pyl3/7/9/11/12* (abbreviated as *3791112*) quintuple mutant. In the *3791112* mutant, PYL3-179insT resulted in a frameshift at codon 60; PYL7-93insA resulted in a nonsense mutation at codon 30; PYL9-Del59-63 resulted in a frameshift at codon 20; PYL11-

Del71-78 resulted in a frameshift at codon 25; and PYL12-Del46-75 resulted in a deletion from codon 16 to 25 (Figure S1C).

Growth Defects of the 112458 379101112 Mutant

Similar to the *snrk2.2/3/6* mutant (Fujii and Zhu, 2009), the *112458 379101112* mutant showed severely impaired growth in soil and could hardly survive under low humidity conditions (Figure 2). In contrast, the *3791112* mutant showed no obvious difference compared with Col-0 WT. Although most of the *112458 379101112* mutant seedling could grow under our growth room conditions (60%–65% relative humidity, 16 hr light/8 hr dark), they were very small, hardly survived after bolting, and failed to produce seeds (Figure 2A, left). The *112458 379101112* mutant seedlings were dwarf plants with small rosettes, short roots, and very reduced biomass (Figures 2B–2G). Their inflorescences frequently wilted and dried, and sometimes quick dehydration happened to whole seedlings (Figure S1D). Although short-day conditions improved the plant height and rosette width of *112458 379101112* and *snrk2.2/3/6* mutants, their total biomass did not increase, since they showed fewer axillary branches under short-day conditions compared to long-day conditions (Figures 2A–2E). When a plastic cover was used to maintain a near dew point humidity, the *112458 379101112* mutant plants grew better and occasionally produced a few seeds. The seedlings and seeds of the *112458 379101112* and *snrk2.2/3/6* mutants were very susceptible to fungal infection under high humidity. When the humidity was reduced to 80%–90% by removing part of the plastic cover, a small amount of seeds could be obtained occasionally (Figures 2A, right, 2H, and S1E). Furthermore, some batches of the *112458 379101112* seeds did not germinate, and the germinated batch did not have the same seed vigor as WT seeds (Figure 2I). Thus, it was extremely difficult to maintain the *112458 379101112* mutant.

Extreme ABA-Insensitive Phenotypes of the 112458 379101112 Mutant

Elegant work of Gonzalez-Guzman et al. showed that the *112458* mutant plants are insensitive to ABA-induced stomatal closure (Gonzalez-Guzman et al., 2012). We noticed that *112458 379101112* mutant plants lost water very quickly when transferred to environments with lower humidity. To avoid the growth retardation of *112458 379101112* plants in soil, we performed water loss and stomatal assays using 25-day-old seedlings grown on agar plates. The excised *3791112* mutant showed similar water loss compared with WT plants, whereas an enhanced water loss was found in the *112458*, *112458 379101112*, and *snrk2.2/3/6* mutants (Figure 3A, upper panel and Figure 3B). By growing the plants in the presence of 200 μM ABA, the shrinking and water loss were obviously reduced in the *112458* mutant, but not in the *112458 379101112* and *snrk2.2/3/6* mutants (Figure 3A, lower panel and Figure 3C). Consistent with the water loss results, stomata of *112458* plants were closed by growing the plants on 200 μM ABA, whereas stomata of *112458 379101112* and *snrk2.2/3/6* plants grown on 200 μM ABA were still widely open (Figures 3D and 3E).

We also analyzed the ABA-induced inhibition of seed germination and seedling growth. The seed germination and root and shoot growth of the *112458*, *112458 379101112*, and *snrk2.2/3/6* mutants were resistant to 100 μM ABA (Figures 3F–3K). Radicle emergence and seedling growth of *112458* plants were slightly reduced by 100 μM ABA. In contrast,

the seed germination of *112458 379101112* and *snrk2.2/3/6* plants was not reduced even under treatment with 100 μM ABA (Figures 3F and 3G). Interestingly, the role of ABA in promoting root growth and total biomass was obvious in *112458 379101112* seedlings (Figures 3H, 3J, and 3K). Although ABA also promoted the root growth of the *112458* mutant, the total biomass of these mutants was not obviously improved by ABA. Consistent with a previous study (Zhao et al., 2016), ABA dramatically reduced the osmotic potential in both Col-0 and *3791112* mutant, but this effect was nearly blocked in the *112458*, *112458 379101112*, and *snrk2.2/3/6* mutants (Figure 3L).

Senescence and Abscission Defects of the 112458 379101112 Mutant

Consistent with our previous findings (Zhao et al., 2016), the *112458*, *112458 379101112*, and *snrk2.2/3/6* mutants were highly insensitive to ABA-induced leaf senescence (Figure 4A). The *112458 379101112* and *snrk2.2/3/6* mutants had an extremely low seed yield (Figure 2H). A very low level of fertilization was observed in these two mutants even when stems and flowers did not wilt (Figure 4B), which could have been caused by male infertility. Similar to the anthers of the *snrk2.2/3/6* mutants, nearly no pollen was released from anthers in most *112458 379101112* mutant flowers (Figure 4C). We also noticed that the abscission of flower organs was delayed in *112458 379101112* and *snrk2.2/3/6* plants (Figure 4B). Further analysis indicated that the abscission of sepals, petals, stamens, and even the stigma was delayed or abolished in *112458 379101112* and *snrk2.2/3/6* plants (Figure 4D). In contrast, stigma abscission was not abolished in pistils of *112458* plants, whereas the anther dehiscence and the flower organ abscission were also delayed in *112458* flowers (Figures 4B–4D). The *3791112* mutant did not show any difference from WT plants in either ABA-induced senescence or anther dehiscence (Figure 4).

Gene Expression Responses to ABA and to Osmotic Stress in the 112458 379101112 Mutant

The *112458 379101112* mutant is the most relevant mutant to analyze ABA-dependent and ABA-independent osmotic stress responses at the present time, because the *snrk2.2/3/6* triple and *snrk2* decuple mutants are affected in both ABA-dependent and -independent pathways (Fujii et al., 2011). When seedlings were treated with 100 μM ABA for 24 hr, 3,024 genes showed altered transcript levels (2-fold or greater, false discovery rate, $p < 0.05$) compared with that of control conditions in WT seedlings, whereas only 356 showed altered expression in the *112458 379101112* mutant after ABA treatment compared with that of control conditions (Figure 5A; Table S2). Among these genes, only 211 genes overlapped between WT seedlings and the *112458 379101112* mutant, indicating that the ABA-induced regulation of the expression of 93% of the genes altered in WT plants was impaired in the *112458 379101112* mutant (Figure 5A). Heatmaps clearly show that nearly all of the transcript level responses to ABA in WT seedlings were diminished in the *112458 379101112* mutant (Figure 5B).

In contrast, transcript level responses to osmotic stress were readily detectable in the *112458 379101112* mutant (Figures 5C and 5D). When seedlings were treated with 300 mM mannitol for 24 hr, 4,609 genes showed altered expression (2-fold or greater, false discovery rate, $p < 0.05$) in WT seedlings, and 3,407 genes were altered in *112458 379101112* plants

compared with that of control conditions (Figure 5C). Among them, 2,132 genes overlapped between WT seedlings and the *112458 379101112* mutant. This indicates that the mannitol-induced regulation of the expression of ~54% of the genes altered in WT plants was impaired in the *112458 379101112* mutant and suggests that these genes must be regulated by osmotic stress in an ABA-dependent manner, since their regulation requires the presence of the ABA receptors (Figure 5C). Osmotic stress may regulate gene expression directly through an ABA-independent activation of SnRK2s, and/or indirectly through the regulation of ABA accumulation and the subsequent ABA signaling. Among the 1,865 genes co-regulated by ABA and mannitol in WT seedlings, 1,036 overlapped with mannitol-regulated genes in the *112458 379101112* mutant (Figure S2). Among those 2,744 genes exclusively regulated by mannitol treatment in WT seedlings, 1,096 overlapped with mannitol-regulated genes in the *112458 379101112* mutant. Among those 1,275 genes regulated by osmotic stress in *112458 379101112* mutant but not in WT plants, 555 were upregulated, indicating that PYLs negatively regulate these genes under osmotic stress (Figure 5C). Gene ontology (GO) analysis showed that biological processes associated with responses to fungus, bacterium, wounding, organic substance, oxidative stress, and jasmonic acid were enriched in the osmotic stress upregulated genes exclusive in the *112458 379101112* mutant (Figure S3). Heatmaps clearly show that only a relatively small percentage of the transcript level responses to osmotic stress was abolished in the *112458 379101112* mutant, and the majority of the responses was maintained, although the levels of up- or downregulation of many of the transcripts were reduced in the mutant (Figure 5D).

In the *112458 379101112* duodecuple mutant, only *PYL6* and *PYL13* are WT alleles. Moreover, PYL13 cannot respond to ABA in inhibiting PP2Cs (Li et al., 2013; Zhao et al., 2013). We found that the expression of *PYL6* was higher in the *112458 379101112* mutant than in WT seedlings, and the downregulation of *PYL6* by ABA was abolished in the *112458 379101112* mutant (Figure 5E). In the *112458 379101112* and *snrk2.2/3/6* mutants, both ABA and osmotic stress failed to induce a group of ABA-dependent responsive genes, including desiccation/dehydration (*RD*) genes such as *RD29B*, several responsive to ABA (*RAB*) genes, such as *RAB18* and *KIN1*, and even the sucrose efflux transporter *SWEET15* (Figures 5E and 5F). In contrast, another group of genes could be substantially induced by osmotic stress but not ABA in the *112458 379101112* and *snrk2.2/3/6* mutants, including the proline biosynthesis gene *P5CS1*, several senescence-associated genes (*SAGs*), such as *SAG13* and *AtNAP*, *RD* genes, such as *RD20* and *RD22*, and *ABFs*, such as *ABI5* (Figures 5G and 5H). We also found that a group of genes that are known as positive regulators of osmotic stress responses were mainly induced by osmotic stress but not ABA, including the plant natriuretic peptide (PNP) gene *PNP-A*, the NAC transcription factor gene *NAC096*, and also several WRKY transcription factor genes, such as *WRKY46* and *ABO3* (Ding et al., 2014; Ren et al., 2010; Wang et al., 2011; Xu et al., 2013). These genes were upregulated in *112458 379101112* and *snrk2.2/3/6* mutant plants under osmotic stress (Figures 5I and 5J). Consistent with these expression profiles, ABA and proline levels increased in the *112458 379101112* mutant after mannitol treatment, and the osmotic potential and seed germination of the *112458 379101112* mutant was reduced after treatment with mannitol but not with ABA (Figures 5K–5N).

Activation of SnRK2s by Osmotic Stress Is Inhibited by PYLs

In order to evaluate the activation of SnRK2s, we performed in-gel kinase assays (Fujii et al., 2011) with proteins extracted from ABA-insensitive mutants upon treatments with ABA and mannitol. The activation of SnRK2s by ABA was abolished in the *112458*, *112458 379101112*, and *snrk2.2/3/6* mutants but not in the *3791112* mutant (Figure 6A). Interestingly, the activation of SnRK2s by osmotic stress (mannitol treatment) was dramatically enhanced in the *112458 379101112* mutant (Figure 6A, lane 14). The enhancement of SnRK2 activation could also be observed in the *112458* mutant under mannitol treatment (Figure 6A, lane 13). To confirm this result and to investigate SnRK2 activation in more *pyl* mutants, we generated antibodies for phosphorylated Ser175 in the activation loop of SnRK2.6 using the peptide SVLHSQPK-pS-TVGTP as antigen. Ser175 phosphorylation is essential for the activation of SnRK2s (Belin et al., 2006; Vlad et al., 2010). The anti-phosphorylation antibodies recognized ABA- and osmotic stress-activated SnRK2s, since the activation loop is conserved among these proteins (Figure 6B). The phosphorylation of this conserved Ser in the activation loop of SnRK2s was induced by ABA in Col-0 and the *3791112* mutant, but not in the *112458*, *112458 379101112*, and *snrk2.2/3/6* mutants (Figure 6B, left panel). Osmotic stress-induced phosphorylation of Ser175 was dramatically enhanced in *112458* and *112458 379101112* mutants (Figure 6B, right panel). These results suggest that the PYLs negatively regulate osmotic-stress-induced activation of SnRK2s *in vivo*. To test whether recombinant PYLs inhibit osmotic-stress-activated SnRK2s, we performed immunoprecipitation-kinase assays using anti-GFP antibodies and osmotic-stress-treated plants expressing GFP-tagged SnRK2.6 (SnRK2.6-GFP). The immunoprecipitated SnRK2.6-GFP from osmotic stress-treated plants phosphorylated histones, and this phosphorylation was reduced by recombinant GST-fused PYL1 and PYL11 but not by recombinant UXS5, used as control (Figure 6C). Moreover, the inhibition of SnRK2.6-GFP activity by PYL1 and PYL11 was not relieved by addition of ABA (Figure 6C). These data show that PYLs can negatively regulate osmotic-stress-induced activation of SnRK2s. Interestingly, the kinase activity of recombinant SnRK2.6 purified from *E. coli* was not inhibited by PYL1 or PYL11 (Figure 6D). This observation suggests that the inhibition of SnRK2s by PYLs may depend on posttranslational modifications of SnRK2s induced by osmotic stress, or on an unidentified factor co-immunoprecipitated with osmotic stress-activated SnRK2s.

Interactions between PYLs and SnRK2s

To further investigate the relationship between PYLs and SnRK2s, we generated transgenic *Arabidopsis* plants expressing tagged PYL5 and PYL9 driven by their respective native promoters (*ProPYLs:PYLs-HA-YFP*). PYL5- and PYL9-associated proteins were isolated using tandem affinity purification (TAP) from extracts of 9-day-old seedlings with or without mannitol or ABA treatment and were identified by mass spectrometry (Table S3). PYL5-associated proteins included PYL4/6/9/10, SnRK2.6, and SnRK2.5 (Figure 7A). PYL9-associated proteins included PYL5/7/8/10, SnRK2.6, −2.5, −2.2, −2.3, −2.4, −2.9, and −2.10 (Figure 7B). Besides the PYLs and SnRK2s, PP2Cs were also co-purified with PYL9, and the association between PYL9 and PP2Cs was enhanced by mannitol and ABA treatment (Figure 7B). These data indicate that PYLs interact with SnRK2s *in vivo*, and their interaction is not altered upon ABA or mannitol treatment. To corroborate these interactions,

we performed split luciferase (LUC) complementation assays in *Nicotiana benthamiana* leaves. We fused PYLs to the N-terminal domain of firefly LUC (PYLs-nLUC) and SnRK2.6 to the C-terminal domain of LUC (SnRK2.6-cLUC), and co-transformed the two constructs using *Agrobacterium* infiltration. LUC activity was detected in leaves co-expressing SnRK2.6-cLUC with PYLs-nLUC or with the positive control ABI1-nLUC, but not with the negative control nLUC (Figures 7C and 7D). The results confirm that PYLs interact with SnRK2s. To further test the interaction between PYLs and SnRK2.6, we fused SnRK2.6 to the GAL4-activation domain (AD) and PYLs to the GAL4 DNA binding domain (BD) and performed yeast two-hybrid assays. We did not find obvious interactions between PYLs and SnRK2s (Figure 7E). These results suggest that PYLs indirectly interact with SnRK2.6, or that their interaction requires protein modifications of SnRK2.6 and/or PYLs *in planta*, or additional factors present in plant cells.

DISCUSSION

Osmotic stress or reduced water availability induce the accumulation of ABA, which is perceived by proteins from the PYL family, activating responses that are critical for plant adaptation to stress and other aspects of growth and development. The previously reported *pyl 1124* (Park et al., 2009) and *112458* (Gonzalez-Guzman et al., 2012; Zhang et al., 2016) mutants have been instrumental to reach our current understanding of ABA receptor function in several aspects of plant growth and development, including stress responses. However, a deeper understanding of the physiological function of the PYL family of ABA receptors requires higher-order mutants defective in additional *PYL* genes. In this study, we generated *pyl* quattuordecuple mutants by mutating all 14 members of the *PYL* family. However, the *pyl* quattuordecuple mutants failed to produce seeds even under very high humidity conditions. We thus characterized in detail a *112458 379101112* duodecuple mutant. In the *112458 379101112* duo-decuple mutant, *PYL13* remains as its WT allele but does not respond to ABA (Li et al., 2013; Zhao et al., 2013). Therefore, only one functional ABA receptor, PYL6, remains in the duodecuple mutant, where the *PYL6* gene is overexpressed in comparison with WT plants (Figure 5E). Approximately 7% of transcript level responses to 100 μM ABA treatment remained in the *112458 379101112* background, presumably due to the overexpression of the *PYL6* allele (Figures 5A and 5E). Although a *pyl6* single mutant does not show obvious differences compared with WT plants (Antoni et al., 2013; Fuchs et al., 2014), the *pyl6 pyl13* double mutant is less sensitive to ABA-induced inhibition of seed germination (Fuchs et al., 2014). Similar to the *snrk2.2/3/6* triple mutant (Fujii and Zhu, 2009), the *112458 379101112* mutant is defective in growth, flower development, and seed production (Figures 1, 2, and 4) and is extremely insensitive to ABA effects on seed germination, seedling growth, stomatal closure, osmotic regulation, leaf senescence, and global regulation of gene expression (Figures 3, 4, and 5). The growth defects of *112458 379101112* and *snrk2.2/3/6* mutants could be alleviated by keeping a near saturation humidity, suggesting that these two mutants suffered from excessive transpiration due to a severe defect in stomatal closure and the less developed roots in these mutants (Figures 2 and 3). The growth defects of these ABA-insensitive mutants could also be alleviated under short-day conditions (Figure 2). Interestingly, the growth of the *112458 379101112* mutant could be promoted by ABA supplementation (Figures 3H–3K), suggesting that PYL6 is still

able to activate ABA signaling and promote plant growth. Compared with the *112458* sextuple mutant, the *112458 379101112* mutant is additionally impaired in growth and seed yield and vigor (Figure 2), and less sensitive to 200 μM ABA in germination, growth, stomatal closure, and water loss (Figure 3). However, the *3791112* quintuple mutant did not show obvious differences compared with WT plants in growth or ABA responses (Figures 2, 3, and 4). These results suggest that PYL3/7/9/10/11/12 are functional, but redundant with PYR1/PYL1/2/4/5/8 in the regulation of these processes. A previous study reported a reduced ABA-induction of leaf yellowing in the *pyl9* single mutant under low light (Zhao et al., 2016), suggesting that PYL9 plays an important role in this response. Taken together, these results suggest that PYL3, PYL7, PYL11, and PYL12 play a minor role in these ABA responses, which is consistent with the extremely low expression of these genes (Gonzalez-Guzman et al., 2012). Overall, our results and results from previous studies (Gonzalez-Guzman et al., 2012; Park et al., 2009) reinforce the notion that PYLs are the major ABA receptors, if not the sole ABA receptors, in higher plants. Although we recovered only one allele of the *pyl 112458 379101112* duodecuple mutant, and we were not able to do complementation experiments with the mutant due to its growth defects and extreme sensitivity to environmental perturbations, we believe that the above phenotypes observed in the *112458 379101112* mutant were caused by the *pyl* mutations, because similar phenotypes were also found in the *snrk2.2/3/6* triple mutant, which is nearly completely insensitive to ABA (Fujii and Zhu, 2009). The results obtained using the *pyl* quattuordecuple and duodecuple mutants, together with those on *snrk2.2/3/6* triple mutants, demonstrate that ABA signaling is critical for growth and development in plants.

Our RNA sequencing (RNA-seq) analysis revealed that ABA-dependent osmotic stress responses were nearly blocked in the *112458 379101112* mutant, whereas the majority of ABA-independent responses remained (Figure 5). This confirms the existence of ABA-independent osmotic stress responses (Fujii et al., 2011). SnRK2s are key components of both ABA-dependent and ABA-independent osmotic stress response pathways (Fujii et al., 2011; Fujii and Zhu, 2009). To our surprise, osmotic-stress-induced activation of SnRK2s was enhanced in *112458 379101112* and *112458* mutants, whereas ABA-induced activation of SnRK2s was blocked in these *pyl* mutants and in *snrk2.2/3/6* mutants (Figure 6). These results reveal that PYLs play a role in antagonizing ABA-independent SnRK2 activity and gene expression and suggest a compensatory mechanism in the regulation of ABA-dependent and -independent osmotic stress responses. In such a case, PYLs could simultaneously promote ABA-dependent responses and repress ABA-independent responses to ensure signal specificity, and their mutation in *112458 379101112* and *112458* mutants would relieve this suppression. Genes related to proline biosynthesis (i.e., *P5CS1*), senescence (i.e., *SAG13* and *AtNAP*), and osmotic responses (i.e., *ABI5*, *RD20*, and *RD22*) were induced by osmotic stress, but not ABA, in *112458 379101112* mutant plants (Figure 5F). This was also the case for other putative ABA-independent osmotic stress-responsive genes (i.e., *NAC096*) (Figure 5G). Osmotic stress may induce the expression of these genes through an ABA-independent pathway, involving the activation of SnRK2s or the accumulation of toxic hydrogen peroxide. These genes are associated with osmotic stress responses: NAC096 directly interacts with ABF2 and ABF4 and synergistically activates stress responsive genes (Xu et al., 2013), WRKY transcription factors, such as WRKY46

and ABO3, positively regulate genes involved in osmotic regulation and redox homeostasis (Ding et al., 2014; Ren et al., 2010), and PNP signaling may participate in regulating osmotic stress responses (Wang et al., 2011). Consistent with these results, ABA accumulation induced by osmotic stress is not affected in the *snrk2.2/3/6* mutant, and proline accumulation is induced by osmotic stress, but not ABA, in the *snrk2.2/3/6* mutant (Fujii et al., 2011). Although ABA-induced leaf senescence was blocked in *112458 379101112* and *snrk2.2/3/6* mutants, age-dependent leaf senescence appeared accelerated in these mutants in soil after bolting (Figures 1B and 2A). Due to their constitutively open stomata, the extremely ABA-deficient or ABA-insensitive mutants (i.e., *aba2-1*, *112458 379101112*, and *snrk2.2/3/6*) suffer from an inadequate water supply even in well-watered soil when the humidity is not near saturation. This appears to activate ABA-independent osmotic stress responses including leaf senescence in these mutants, but not in WT plants.

Osmotic stress, but not ABA, activates subclass I SnRK2s (SnRK2.1/2.4/2.5/2.9/2.10). These genes apparently evolved later than ABA-activated subclass III SnRK2s (SnRK2.2/2.3/2.6) (Lind et al., 2015). Although the activation of SnRK2s by osmotic stress was enhanced in *112458* and *112458 379101112* mutants (Figures 6A and 6B), we observed neither an induction of stomatal closure nor an induction of ABA-dependent osmotic-stress-responsive genes in *112458 379101112* under osmotic stress conditions (Figure 5E). These results indicate that the substrates of osmotic-stress-activated SnRK2s are quite different from those of the ABA-activated SnRK2s. Besides ABFs, other transcription factors such as ANAC096, WRKY6, WRKY57, and ABO3 also positively regulate osmotic stress responses (Huang et al., 2016; Jiang et al., 2012; Xu et al., 2013), but these other transcription factors may not be substrates of SnRK2s. Thus, the activation of SnRK2s is essential but may not be sufficient to initiate general osmotic stress responses.

We discovered that PYLs interact with SnRK2s *in vivo* and negatively regulate osmotic stress activation of SnRK2s (Figures 6A and 6B). We found that recombinant PYLs inhibit the activity of immunoprecipitated osmotic-stress-activated SnRK2.6-GFP, but do not inhibit the activity of recombinant SnRK2.6 from *E. coli* (Figures 6C and 6D). Among the ABA-deficient or -insensitive mutants, *pyl* mutants, but not *aba1-3*, *abi1-1*, or *snrk2.2/3/6*, show an enhanced activation of SnRK2s by osmotic stress (Boudsocq et al., 2007; Fujii et al., 2011). This suggests that PYLs may inhibit osmotic stress activation of SnRK2s in a manner that is independent of the core ABA signaling. Further investigation indicated that the physical association with and inhibition of SnRK2s by PYLs may depend on protein modifications of SnRK2s *in vivo* (e.g., phosphorylation induced by osmotic stress), or unidentified components of osmotic stress signaling (Figures 6 and 7). Recent studies suggest that, besides the clade A PP2Cs, members of other protein phosphatase families also regulate the activity of SnRK2s (Hou et al., 2016; Waadt et al., 2015), supporting the notion that a complex network exists for the regulation of SnRK2 activities.

STAR+METHODS

KEY RESOURCES TABLE

REAGENT or RESOURCE	SOURCE	IDENTIFIER
Antibodies		
Anti-phosphorylation antibodies for Ser175 in SnRK2.6	Yun-de-ZymTM antibodies, LLC (South San Francisco, CA)	Antigen: SVLHSQPK-pS-TVGTP
Mouse monoclonal anti-GFP	Sigma-Aldrich	Cat#11814460001
Rabbit polyclonal anti-Actin	Abcam	Cat#ab197345
Goat Anti-Mouse IgG (H+L)-HRP Conjugate	Bio-rad	Cat#172-1011
Goat Anti-rabbit IgG (H+L)-HRP Conjugate	Bio-rad	Cat#172-1019
Chemicals, Peptides, and Recombinant Proteins		
Abscisic Acid	Sigma-Aldrich	Cat#A1049
D-Mannitol	Sigma-Aldrich	Cat#M4125
Leupeptin	Sigma-Aldrich	Cat#11017101001
Aprotinin	Sigma-Aldrich	Cat#10236624001
Antipain	Sigma-Aldrich	Cat#10791
cOmplete, EDTA-free Protease Inhibitor Cocktail	Roche	Cat#04693132001
HA peptide	Abcam	Cat#ab13835
ATP, [γ-32P]-6000Ci/mmol	PerkinElmer	NEG502Z500UC
Firefly D-luciferin	NanoLight	CAS#2591-17-5
Critical Commercial Assays		
ECL Prime Western Blotting System	GE	Cat#RPN2232
Monoclonal anti-HA agarose with antibody produced in mouse	Sigma-Aldrich	Cat#A2095
GFP-Trap Agarose	Chromotek	Cat#gta-20
Micro Bio-Spin Columns with Bio-Spin® Gel P-6	Bio-rad	Cat#732-6221
Trizol reagent	ThermoFisher Scientific	Cat#15596026
TURBO DNA-free Kit	Ambion	Cat#AM1907
M-MLV Reverse Transcriptase	Promega	Cat#M1705
Ni-NTA Agarose	QIAGEN	Cat#30210
Glutathione Sepharose 4B	GE Healthcare	Cat#17-0756-01
Deposited Data		
Raw and processed RNA sequencing data	GEO (Gene Expression Omnibus) https://www.ncbi.nlm.nih.gov/geo/	GEO: GSE114379
Experimental Models: Organisms/Strains		
E. coli BL21	N/A	N/A
Agrobacterium tumefaciens (strain GV3101)	N/A	N/A
Yeast strain AH109	N/A	N/A
Arabidopsis: WT Col-0	N/A	N/A

REAGENT or RESOURCE	SOURCE	IDENTIFIER
Arabidopsis: pyl quattuordecuple	This study	N/A
Arabidopsis: pyl1124583791011112	This study	N/A
Arabidopsis: pyl13791112 quintuple	This study	N/A
Arabidopsis: pyr1pyl12458	Gonzalez-Guzman et al., 2012	N/A
Arabidopsis: snrk2.2/2.3/2.6	Fujii and Zhu, 2009	N/A
Arabidopsis: SnRK2.6-GFP	Wang et al., 2015	N/A
Arabidopsis: ProPYL5:PYL5-HA-YFP in *pyr1pyl1/2/3*	This study	N/A
Arabidopsis: ProPYL9:PYL9-HA-YFP in *pyr1pyl1/2/3*	This study	N/A
Oligonucleotides		
Primers used in this study	This study; Table S1	N/A
Recombinant DNA		
Vector A-6× sgR-PYL3,6,7,9,11,12-Cas9	This study	N/A
Vector B-2× sgR-PYL10,13-Cas9	This study	N/A
Vector C-2× sgR-PYL6,13-Cas9	This study	N/A
ProPYL5:PYL5-HA-YFP	This study	N/A
ProPYL9:PYL9-HA-YFP	This study	N/A
pMal-c2X-SnRK2.6	Fujii et al., 2009	N/A
GST-ABF	Fujii et al., 2009	Gly 73 to Gln 119
pGEX-4T1-PYL1	This study	N/A
pGEX-6P1-PYL11	Hou et al., 2016	N/A
pGEX-6P1-UXS5	This study	N/A
pET28a-PYL1	This study	N/A
pET28a-PYL11	Hou et al., 2016	N/A
PYR1-nLUC	This study	N/A
PYL1-nLUC	This study	N/A
PYL2-nLUC	This study	N/A
PYL3-nLUC	This study	N/A
PYL4-nLUC	This study	N/A
PYL5-nLUC	This study	N/A
PYL6-nLUC	This study	N/A
PYL7-nLUC	This study	N/A
PYL8-nLUC	Zhao et al., 2014	N/A
PYL9-nLUC	This study	N/A
PYL10-nLUC	This study	N/A
PYL11-nLUC	Hou et al., 2016	N/A
PYL12-nLUC	This study	N/A
PYL13-nLUC	This study	N/A
SnRK2.6-cLUC	Yan et al., 2017	N/A

REAGENT or RESOURCE	SOURCE	IDENTIFIER
pGAL4-BD-PYR1	Park et al., 2009	N/A
pGAL4-BD-PYL1	Park et al., 2009	N/A
pGAL4-BD-PYL2	Park et al., 2009	N/A
pGAL4-BD-PYL3	Park et al., 2009	N/A
pGAL4-BD-PYL4	Park et al., 2009	N/A
pGAL4-BD-PYL5	Park et al., 2009	N/A
pGAL4-BD-PYL6	Park et al., 2009	N/A
pGAL4-BD-PYL7	Park et al., 2009	N/A
pGAL4-BD-PYL8	Park et al., 2009	N/A
pGAL4-BD-PYL9	Park et al., 2009	N/A
pGAL4-BD-PYL10	Park et al., 2009	N/A
pGAL4-BD-PYL11	Park et al., 2009	N/A
pGAL4-BD-PYL12	Park et al., 2009	N/A
pGAL4-BD-PYL13	Park et al., 2009	N/A
pGADT7-SnRK2.6	This study	N/A
Software and Algorithms		
ImageJ	ImageJ	https://imagej.nih.gov/ij/
GraphPad Prism	GraphPad Software	https://www.graphpad.com/

CONTACT FOR REAGENT AND RESOURCE SHARING

Further information and requests for resources and reagents should be directed to and will be fulfilled by the Lead Contact, Jian-Kang Zhu (jkzhu@purdue.edu).

EXPERIMENTAL MODEL AND SUBJECT DETAILS

All plants are in the Col-0 background. Plants were grown at 23°C under a 16/8 hr light/dark photoperiod with 60%–70% relative humidity unless indicated.

METHOD DETAILS

Generation of the 112458 379101112 Mutant—The constructs for CRISPR were designed according to the protocol described previously (Zhang et al., 2016). We constructed two CRISPR/Cas9 vectors to edit the remaining *PYLs* in the *112458* sextuple mutant background (Gonzalez-Guzman et al., 2012). Vector A targets *PYL3/6/7/9/11/12* genes with six sgRNAs and a hygromycin resistance gene. Vector B targets *PYL10/13* with two sgRNAs and a kanamycin resistance gene. The arrangement of these sgRNAs in these two CRISPR/Cas9 constructs is shown in Figure S1A. The sequences of the synthesized guide oligos are shown in Table S1.

Vector A and vector B were co-transformed into the *112458 pyl* T-DNA mutant using agrobacterium-mediated co-transformation. All transgenic plants were screened for hygromycin and kanamycin resistance with 30 mg/L hygromycin and 50 mg/L kanamycin

plus 50 mg/L carbenicillin. The surviving T1 plants were transplanted to soil after growing under long-day conditions (16 h light/8 h dark) at 22°C for 2 weeks.

Thirty individual T1 transformants were analyzed by sequencing their *PYL* target regions, which were amplified by PCR using primer pairs listed in Table S1. Mutations on targeted genes were detected by aligning the sequencing chromatograms of these PCR products with the WT controls. We detected mutations in seven *PYLs* including *PYL3/7/9/10/11/12/13* in line #20. Then we used 48 individuals from T2 segregation of line #20 and generated the homozygous *pyr1pyl1/2/4/5/8/3/7/11/12* decuple mutant (line #20-43), in which *PYL9* and *PYL10* are heterozygous. We then used 12 individuals from the T3 segregation of line #20-43 and generated the homozygous *pyr1pyl1/2/4/5/8/3/7/10/11/12* hendecuple mutant, in which *PYL9* is heterozygous. Finally we generated the *112458 379101112* duodecuple mutant in the T4 generation (Figure S1B).

Generation of pyl Quattuordecuple Mutants—We constructed vector C to edit *PYL6* and *PYL13* in the *112458* sextuple mutant background. Vector C targets *PYL6/13* with two sgRNAs and a hygromycin resistance gene. The gRNA oligo ‘‘GCTGATGTGCCGGAGCACGTGG’’ was selected for *PYL6* and the gRNA oligo ‘‘CGTGGTGGATGTGCCGGAAGG’’ was selected for *PYL13* (Figure S1B).

Vector C was transformed into the *112458 pyl* T-DNA mutant using *Agrobacterium*-mediated transformation. All transgenic plants were screened for hygromycin resistance with 30 mg/L hygromycin plus 50 mg/L carbenicillin. The surviving T1 plants were transplanted to soil after growing under long-day conditions (16 h light/8 h dark) at 22°C for 2 weeks.

Twenty individual T1 transformants were analyzed by sequencing their *PYL6* and *PYL13* target regions, which were amplified by PCR using primer pairs listed in Table S1. We detected mutation in *PYL13* in four lines, but no *PYL6* mutation was detected in T1 lines. From 37 individual T2 segregations of these four lines, we detected mutation in *PYL6*. Then we generated the homozygous *pyr1pyl1/2/4/5/8/6/13* octuple mutant.

We crossed *pyr1pyl1/2/4/5/8/6/13* octuple mutant with the *112458 379101112* duodecuple mutant. We screened thousands of F2 seedlings and finally obtained the *pyl* quattuordecuple mutants.

Plant Growth Conditions—Seeds were sterilized for 10 min in 20% bleach and then rinsed four times in sterile-deionized water. Sterilized seeds were grown horizontally on 0.3% Phytagel (Sigma) or vertically on 0.6% Phytagel medium containing 1/2 MS nutrients (PhytoTech), 1% sucrose, pH5.7, and kept at 4–8°C for 3 days. For ABA related analysis, 1 g/L MES buffer anhydrous (Amresco, E183) was added before autoclaving to prevent acidification of ABA. ABA (Sigma, A1049) was added to the cooled, autoclaved medium prior to pouring plates. Seedlings were grown in a Percival CU36L5 incubator at 23°C under a 16-h light/8-h dark photoperiod. Seedlings were grown vertically for 4 d before transfer to medium with or without the indicated concentrations of ABA or mannitol. *Arabidopsis* plants were grown in soil (Fafard Super Fine Germination Mix) in a growth room at 22°C

under a 60%–65% relative humidity and a 16-h light/8-h dark photoperiod. For *pyl* decuple, hendecuple, duodecuple mutants and *snrk2.2/3/6* triple mutant, seedlings were partially covered with stackable plastic covers to maintain 80%–90% humidity (Figure S1E) and were watered every two days.

Measurement of Water Loss and Stomatal Assay—We used 25-d-old seedlings grown on 1/2 MS plates to avoid the serious growth retardation of extreme ABA-insensitive mutants. These seedlings were grown on 1/2 MS plates for 5-days. And then transferred to 1/2 MS plates (0.3% Phytagel) with or without 200 μM ABA and grown horizontally for 20 days. Seedlings were spaced 3 cm apart. Whole rosettes of 25-d-old plants were cut from the base and weighted at indicated time points. Stomatal apertures were measured in rosette leaves of 25-d-old plants using a ZEISS AX10 microscope.

Osmotic Potential Measurements—Osmotic potential was measured as previously reported (Zhao et al., 2016). For Figure 3L, osmotic potentials were analyzed 11 d after the 4-d-old seedlings were transferred to medium with indicated concentrations of ABA. For Figure 5H, osmotic potentials were analyzed after 24 h treatment with 30 μM ABA or 400 mM mannitol.

Measurement of ABA and Proline Assay—For quantification of ABA and proline, tissues were ground in liquid nitrogen. ABA concentration was measured with by UPLC-MS/MS method (Balcke et al., 2012). ABA level was analyzed 12 hour after the 9-d-old seedlings were transferred to medium with 200 mM mannitol. Proline was assayed using the ninhydrin-based colorimetric assay as reported (Bates et al., 1973). Proline level were analyzed 24 hour after the 9-d-old seedlings were transferred to filter papers with 400 mM mannitol or 30 μM ABA.

RNA Sequencing and Real-Time PCR—Seedlings were grown vertically for 9 days before treatment. These seedlings (0.05 ~0.1 g) were mock treated, or treated with 100 μM ABA or 300 mM mannitol for 24 hours on filter papers. Total RNA was extracted with Trizol reagent (ThermoFisher Scientific, 15596026). The library construction and sequencing were performed in the Genomics Core Facilities of the Shanghai Center for Plant Stress Biology, CAS (Shanghai, China) with Illumina HiSeq2500. The expression data of genes analyzed is listed in Table S2. Real-time PCR was performed as previously reported (Zhao et al., 2016).

Reads of RNA-seq data were mapped to *Arabidopsis* reference genome (TAIR10) using TopHat (Trapnell et al., 2012). Differentially expressed genes (DEG) were identified using cuffdiff in Cufflinks. We define a gene as DEG by requiring q-value < 0.05 and at least 2 fold change of expression level.

In-gel Kinase Assay—The in-gel kinase assay were performed as previously described (Wang et al., 2018). We used 20-μg total proteins for each sample and histone as substrate. Ten-day-old seedlings grown on 1/2 MS medium with 1% sucrose were transferred into liquid MS medium, or medium with 50 μM ABA, and 0.5 M mannitol for 30 min. After electrophoresis, the gel was dried under vacuum at 80°C for 1.5 hour on filter paper and

exposed to a phosphor imager for 3 days. Radioactivity was detected with a Personal Molecular Imager (Bio-Rad, Hercules, CA).

Generation of Anti-phosphorylation Antibodies and Immunoblotting—The generation of anti-phosphorylation rabbit antibody was performed in the Yun-de-ZymTM antibodies, LLC (South San Francisco, CA). The HPLC high purity modified peptide CSVLHSQPK-pS-TVGTP-amide was used as antigen to generate polyclonal anti-phosphorylation antibody for Ser175 in SnRK2.6. The antibody was purified using modified-peptide conjugated affinity matrix. The phosphorylation-site-specific antibody was purified using non-modified peptide CSVLHSQPKSTVGTP-amide, which absorbs the phosphorylation-site-nonspecific antibody.

For extraction of total protein from plants, we used an extraction buffer containing 100 mM HEPES, pH 7.8, 5 mM EDTA, 5 mM EGTA, 10 mM Na_3VO_4, 10 mM NaF, 50 mM Glycero-P, 10 mM DTT, 10 μg/ml Leupeptin, 10 μg/ml Antipain, 10 μg/ml Aprotinin, 1 mM PMSF, and 5% Glycerol. Samples were ground in extraction buffer and centrifuged at 4°C for 40 min at 13,500 rpm. The total protein in supernatants was determined with the Bradford method. We used 20-μg total proteins for each sample for in-gel assay and 40-μg total proteins for western blots.

Western blots were performed as described (Zhao et al., 2013). We incubated the membranes at 4°C overnight in PBS-T with 1% skim milk containing 1:1000 diluted anti-phosphorylation antibodies for Ser175 in SnRK2.6. After they were washed five times (5 min each) with PBST, membranes were incubated for 1 h at room temperature in PBS-T with 1% skim milk containing 1:2000 diluted goat anti-rabbit HRP-conjugated antibodies (Pierce, 32460), and then washed and detected using Lumi-Light Western Blotting Substrate (Roche) with 10–60 min exposure.

Immunoprecipitation (IP) Kinase Assay—The immunoprecipitation kinase assays of SnRK2.6-GFP kinase were performed as previously described with some modification (Boudsocq et al., 2004). Ten-day-old *ost1*/*SnRK2.6-GFP* seedlings were treated with or without 0.5 M mannitol for 30 min. Samples (1 g) were collected and grounded in liquid nitrogen. Total protein was extracted in 4 mL IP-buffer (10 mM Tris-HCl, pH 7.5, 150 mM NaCl, 0.5 mM EDTA, 1 mM NaF, 1 mM Na_4VO_3, 10 mM β-glycerophosphate, 0.5% NP-40, with protease inhibitor). After centrifuged at 20,000 g for 20 min, the supernatants were incubated with 20 μL GFP-trap for 4 hours at 4°C. After incubation, the beads were washed with IP-buffer for 2 times, washing buffer (10 mM Tris-HCl, pH 7.5, 300 mM NaCl, 0.5 mM EDTA, 1 mM NaF, 1 mM Na_4VO_3, 10 mM β-glycerophosphate, 0.5% NP-40, with protease inhibitor) for 2 times, and kinase buffer (25 mM Tris-HCl, pH 7.5, 10 mM $MgCl_2$, 0.25 mM DTT) for 1 time. Two μL aliquot of GFP-trap was incubated with 0.2 μg of GST-PYL1, GST-PYL11, GST-UXS5 or GST elution buffer (25 mM Tris-HCl, pH 7.5, 10 mM GSH) for 20 min at room temperature. After incubation, 2 μg histone and hot ATP were added to the reaction and incubated for additional 90 min at room temperature. The proteins were separated by SDS-PAGE. After electrophoresis, the gel was dried under vacuum at 80°C for 1.5 hour on filter paper and exposed to a phosphor imager for 10 h.

In vitro Kinase Assay—His tagged PYL proteins were desalted using Micro Bio-Spin Columns with Bio-Spin® Gel P-6 (Catalog #732-6221). MBP-SnRK2.6 (0.5 μg) was incubated with HIS tagged PYL proteins (0.5–1.5 μg) with or without 5 μM ABA in 20 μL reaction buffer (50 mM Tris-HCl pH 7.0, 20 mM $MgCl_2$, 0.1 mM EGTA and 0.1% β-mercaptoethanol) at room temperature. After incubated for 30 min, 1 μM ATP, 4 μg GST-ABF2 and 5 μCi[γ-^{32}P]ATP were added to the reaction. After incubated at room temperature for 30 min, proteins were separated by SDS-PAGE. After electrophoresis, the gel was dried under vacuum at 80°C for 1.5 hour on filter paper and exposed to a phosphor imager for 2 h. Radioactivity was detected with a Personal Molecular Imager (Bio-Rad, Hercules, CA).

Tandem affinity purification—To generate the *ProPYLs:PYLs-HA-YFP* constructs, the promoter fragments of *PYLs* was cloned into the SalI and *BamH*I sites of the modified pSAT vector with YFP and 3HA tags at the C terminus. The coding region of *PYLs* was cloned between the *PYL* promoter and the *YFP* sequence. The whole insertion cassette was digested with *PI-Psp*1 and inserted into pRCS2-htp binary plasmids. These plasmids were transformed into *pyr1pyl1/2/3*. Transgenic plants were verified by western blot assay.

The tandem affinity purification was performed as previously described (Zhao et al., 2016). The transgenic *Arabidopsis* plants expressing *ProPYLs:PYLs-HA-YFP* were used for tandem affinity purification (TAP). Ten-day-old seedlings (3–4 g fresh weight) were soaked for 30 min with or without 0.8 M mannitol. Generally, proteins were pre-purified with monoclonal anti-HA agarose with antibody produced in mouse (A2095, Sigma) in IP buffer (50 mM Tris-HCl, pH 7.5, 150 mM NaCl, 1 mM EDTA, 0.1% NP-40, 1 x protease cocktail, Roche), and eluted by HA peptide (Abcam, ab13835) with a concentration of 0.5 μg/μL in 200 μL IP buffer. PYLs-HA-YFP and their interacting proteins were then affinity purified with GFP-Trap Agarose (Chromotek, gta-20) and identified by mass spectrometric (MS) analyses. All steps were performed at 4°C.

The sequence of the peptides is listed in Table S3.

Split luciferase (LUC) complementation assay—The coding sequence of *PYLs* was amplified by PCR, cloned into pENTR vectors and transferred to pEarley-nLUC/cLUC vectors through LR reactions. Split-LUC complementation assay was performed by transient expression in tobacco leaves through agrobacterium-mediated infiltration as previously described (Hou et al., 2016). Two days after infiltration, luciferase activity was detected with a CCD camera by applying firefly D-luciferin (NanoLight).

Yeast Two Hybrid Assay—pBD-GAL4-PYLs were as reported (Park et al., 2009). *Saccharomyces cerevisiae* AH109 cells were transformed with pGADT7-SnRK2.6 and pBD-GAL4-PYLs plasmids. Colonies were identified on yeast SD medium lacking Leu and Trp and transferred to selective SD medium lacking Leu, Trp and His. To determine the interaction intensity, dilutions of saturated yeast cultures (10^{-1}, 10^{-2} and 10^{-3}) were spotted onto selection medium. Photographs were taken after 5 days incubation at 28° C.

QUANTIFICATION AND STATISTICAL ANALYSIS

Radioactivity quantification of bands in in-gel and immunoprecipitation kinase assays was performed using ImageJ. Student's t test was used to determine the statistical significance between wild-type and mutants in assays related to germination, rosette width, root length, fresh weight, osmotic potential, and relative intensity (*$p < 0.05$).

DATA AND SOFTWARE AVAILABILITY

The accession number for the raw and processed RNA sequencing data reported in this paper is GEO: GSE114379.

Supplementary Material

Refer to Web version on PubMed Central for supplementary material.

Acknowledgments

This work was supported by the Chinese Academy of Sciences and by NIH grant R01GM059138 (to J.-K.Z.). We are grateful to Prof. Pedro Rodriguez of Universidad Politecnica de Valenci, Spain, for kindly providing the *pyr1pyl12458* mutant seeds.

References

Antoni R, Gonzalez-Guzman M, Rodriguez L, Rodrigues A, Pizzio GA, Rodriguez PL. Selective inhibition of clade A phosphatases type 2C by PYR/PYL/RCAR abscisic acid receptors. Plant Physiol. 2012; 158:970–980. [PubMed: 22198272]

Antoni R, Gonzalez-Guzman M, Rodriguez L, Peirats-Llobet M, Pizzio GA, Fernandez MA, De Winne N, De Jaeger G, Dietrich D, Bennett MJ, Rodriguez PL. PYRABACTIN RESISTANCE1-LIKE8 plays an important role for the regulation of abscisic acid signaling in root. Plant Physiol. 2013; 161:931–941. [PubMed: 23370718]

Balcke GU, Handrick V, Bergau N, Fichtner M, Henning A, Stellmach H, Tissier A, Hause B, Frolov A. An UPLC-MS/MS method for highly sensitive high-throughput analysis of phytohormones in plant tissues. Plant Methods. 2012; 8:47. [PubMed: 23173950]

Bates LS, Waldren RP, Teare ID. Rapid determination of free proline for water-stress studies. Plant Soil. 1973; 39:205–207.

Belin C, de Franco PO, Bourbousse C, Chaignepain S, Schmitter JM, Vavasseur A, Giraudat J, Barbier-Brygoo H, Thomine S. Identification of features regulating OST1 kinase activity and OST1 function in guard cells. Plant Physiol. 2006; 141:1316–1327. [PubMed: 16766677]

Bhaskara GB, Nguyen TT, Verslues PE. Unique drought resistance functions of the highly ABA-induced clade A protein phosphatase 2Cs. Plant Physiol. 2012; 160:379–395. [PubMed: 22829320]

Boudsocq M, Barbier-Brygoo H, Laurière C. Identification of nine sucrose nonfermenting 1-related protein kinases 2 activated by hyperosmotic and saline stresses in Arabidopsis thaliana. J Biol Chem. 2004; 279:41758–41766. [PubMed: 15292193]

Boudsocq M, Droillard MJ, Barbier-Brygoo H, Laurière C. Different phosphorylation mechanisms are involved in the activation of sucrose non-fermenting 1 related protein kinases 2 by osmotic stresses and abscisic acid. Plant Mol Biol. 2007; 63:491–503. [PubMed: 17103012]

Cutler SR, Rodriguez PL, Finkelstein RR, Abrams SR. Abscisic acid: Emergence of a core signaling network. Annu Rev Plant Biol. 2010; 61:651–679. [PubMed: 20192755]

Ding ZJ, Yan JY, Xu XY, Yu DQ, Li GX, Zhang SQ, Zheng SJ. Transcription factor WRKY46 regulates osmotic stress responses and stomatal movement independently in Arabidopsis. Plant J. 2014; 79:13–27. [PubMed: 24773321]

Dupeux F, Santiago J, Betz K, Twycross J, Park SY, Rodriguez L, Gonzalez-Guzman M, Jensen MR, Krasnogor N, Blackledge M, et al. A thermodynamic switch modulates abscisic acid receptor sensitivity. EMBO J. 2011; 30:4171–4184. [PubMed: 21847091]

Fuchs S, Tischer SV, Wunschel C, Christmann A, Grill E. Abscisic acid sensor RCAR7/PYL13, specific regulator of protein phosphatase coreceptors. Proc Natl Acad Sci USA. 2014; 111:5741–5746. [PubMed: 24706923]

Fujii H, Zhu JK. Arabidopsis mutant deficient in 3 abscisic acid-activated protein kinases reveals critical roles in growth, reproduction, and stress. Proc Natl Acad Sci USA. 2009; 106:8380–8385. [PubMed: 19420218]

Fujii H, Chinnusamy V, Rodrigues A, Rubio S, Antoni R, Park SY, Cutler SR, Sheen J, Rodriguez PL, Zhu JK. In vitro reconstitution of an abscisic acid signalling pathway. Nature. 2009; 462:660–664. [PubMed: 19924127]

Fujii H, Verslues PE, Zhu JK. Arabidopsis decuple mutant reveals the importance of SnRK2 kinases in osmotic stress responses in vivo. Proc Natl Acad Sci USA. 2011; 108:1717–1722. [PubMed: 21220313]

Furihata T, Maruyama K, Fujita Y, Umezawa T, Yoshida R, Shinozaki K, Yamaguchi-Shinozaki K. Abscisic acid-dependent multisite phosphorylation regulates the activity of a transcription activator AREB1. Proc Natl Acad Sci USA. 2006; 103:1988–1993. [PubMed: 16446457]

Gonzalez-Guzman M, Pizzio GA, Antoni R, Vera-Sirera F, Merilo E, Bassel GW, Fernández MA, Holdsworth MJ, Perez-Amador MA, Kollist H, Rodriguez PL. Arabidopsis PYR/PYL/RCAR receptors play a major role in quantitative regulation of stomatal aperture and transcriptional response to abscisic acid. Plant Cell. 2012; 24:2483–2496. [PubMed: 22739828]

Hao Q, Yin P, Li W, Wang L, Yan C, Lin Z, Wu JZ, Wang J, Yan SF, Yan N. The molecular basis of ABA-independent inhibition of PP2Cs by a subclass of PYL proteins. Mol Cell. 2011; 42:662–672. [PubMed: 21658606]

He Y, Hao Q, Li W, Yan C, Yan N, Yin P. Identification and characterization of ABA receptors in Oryza sativa. PLoS ONE. 2014; 9:e95246. [PubMed: 24743650]

Hou YJ, Zhu Y, Wang P, Zhao Y, Xie S, Batelli G, Wang B, Duan CG, Wang X, Xing L, et al. Type one protein phosphatase 1 and its regulatory protein inhibitor 2 negatively regulate ABA signaling. PLoS Genet. 2016; 12:e1005835. [PubMed: 26943172]

Huang Y, Feng CZ, Ye Q, Wu WH, Chen YF. Arabidopsis WRKY6 transcription factor acts as a positive regulator of abscisic acid signaling during seed germination and early seedling development. PLoS Genet. 2016; 12:e1005833. [PubMed: 26829043]

Jiang Y, Liang G, Yu D. Activated expression of WRKY57 confers drought tolerance in Arabidopsis. Mol Plant. 2012; 5:1375–1388. [PubMed: 22930734]

Li W, Wang L, Sheng X, Yan C, Zhou R, Hang J, Yin P, Yan N. Molecular basis for the selective and ABA-independent inhibition of PP2CA by PYL13. Cell Res. 2013; 23:1369–1379. [PubMed: 24165892]

Lind C, Dreyer I, Löpez-Sanjurjo EJ, von Meyer K, Ishizaki K, Kohchi T, Lang D, Zhao Y, Kreuzer I, Al-Rasheid KA, et al. Stomatal guard cells co-opted an ancient ABA-dependent desiccation survival system to regulate stomatal closure. Curr Biol. 2015; 25:928–935. [PubMed: 25802151]

Ma Y, Szostkiewicz I, Korte A, Moes D, Yang Y, Christmann A, Grill E. Regulators of PP2C phosphatase activity function as abscisic acid sensors. Science. 2009; 324:1064–1068. [PubMed: 19407143]

Mosquna A, Peterson FC, Park SY, Lozano-Juste J, Volkman BF, Cutler SR. Potent and selective activation of abscisic acid receptors in vivo by mutational stabilization of their agonist-bound conformation. Proc Natl Acad Sci USA. 2011; 108:20838–20843. [PubMed: 22139369]

Munemasa S, Hauser F, Park J, Waadt R, Brandt B, Schroeder JI. Mechanisms of abscisic acid-mediated control of stomatal aperture. Curr Opin Plant Biol. 2015; 28:154–162. [PubMed: 26599955]

Park SY, Fung P, Nishimura N, Jensen DR, Fujii H, Zhao Y, Lumba S, Santiago J, Rodrigues A, Chow TF, et al. Abscisic acid inhibits type 2C protein phosphatases via the PYR/PYL family of START proteins. Science. 2009; 324:1068–1071. [PubMed: 19407142]

Ren X, Chen Z, Liu Y, Zhang H, Zhang M, Liu Q, Hong X, Zhu JK, Gong Z. ABO3, a WRKY transcription factor, mediates plant responses to abscisic acid and drought tolerance in Arabidopsis. Plant J. 2010; 63:417–429. [PubMed: 20487379]

Tischer SV, Wunschel C, Papacek M, Kleigrewe K, Hofmann T, Christmann A, Grill E. Combinatorial interaction network of abscisic acid receptors and coreceptors from *Arabidopsis thaliana*. Proc Natl Acad Sci USA. 2017; 114:10280–10285. [PubMed: 28874521]

Trapnell C, Roberts A, Goff L, Pertea G, Kim D, Kelley DR, Pimentel H, Salzberg SL, Rinn JL, Pachter L. Differential gene and transcript expression analysis of RNA-seq experiments with TopHat and Cufflinks. Nat Protoc. 2012; 7:562–578. [PubMed: 22383036]

Vlad F, Droillard MJ, Valot B, Khafif M, Rodrigues A, Brault M, Zivy M, Rodriguez PL, Merlot S, Laurière C. Phosphosite mapping, genetic and in planta activation studies reveal key aspects of the different phosphorylation mechanisms involved in activation of SnRK2s. Plant J. 2010; 63:778–790. [PubMed: 20561261]

Waadt R, Manalansan B, Rauniyar N, Munemasa S, Booker MA, Brandt B, Waadt C, Nusinow DA, Kay SA, Kunz HH, et al. Identification of Open Stomata1-Interacting Proteins Reveals Interactions with Sucrose Non-fermenting1-Related Protein Kinases2 and with Type 2A Protein Phosphatases That Function in Abscisic Acid Responses. Plant Physiol. 2015; 169:760–779. [PubMed: 26175513]

Wang YH, Gehring C, Irving HR. Plant natriuretic peptides are apoplastic and paracrine stress response molecules. Plant Cell Physiol. 2011; 52:837–850. [PubMed: 21478192]

Wang P, Du Y, Hou YJ, Zhao Y, Hsu CC, Yuan F, Zhu X, Tao WA, Song CP, Zhu JK. Nitric oxide negatively regulates abscisic acid signaling in guard cells by S-nitrosylation of OST1. Proc Natl Acad Sci USA. 2015; 112:613–618. [PubMed: 25550508]

Wang P, Zhao Y, Li Z, Hsu CC, Liu X, Fu L, Hou YJ, Du Y, Xie S, Zhang C, et al. Reciprocal regulation of the TOR kinase and ABA receptor balances plant growth and stress response. Mol Cell. 2018; 69:100–112. [PubMed: 29290610]

Xu ZY, Kim SY, Hyeon Y, Kim DH, Dong T, Park Y, Jin JB, Joo SH, Kim SK, Hong JC, et al. The Arabidopsis NAC transcription factor ANAC096 cooperates with bZIP-type transcription factors in dehydration and osmotic stress responses. Plant Cell. 2013; 25:4708–4724. [PubMed: 24285786]

Yan J, Wang P, Wang B, Hsu CC, Tang K, Zhang H, Hou YJ, Zhao Y, Wang Q, Zhao C, et al. The SnRK2 kinases modulate miRNA accumulation in Arabidopsis. PLoS Genet. 2017; 13:e1006753. [PubMed: 28419088]

Yin P, Fan H, Hao Q, Yuan X, Wu D, Pang Y, Yan C, Li W, Wang J, Yan N. Structural insights into the mechanism of abscisic acid signaling by PYL proteins. Nat Struct Mol Biol. 2009; 16:1230–1236. [PubMed: 19893533]

Zhang Z, Mao Y, Ha S, Liu W, Botella JR, Zhu JK. A multiplex CRISPR/Cas9 platform for fast and efficient editing of multiple genes in Arabidopsis. Plant Cell Rep. 2016; 35:1519–1533. [PubMed: 26661595]

Zhao Y, Chan Z, Xing L, Liu X, Hou YJ, Chinnusamy V, Wang P, Duan C, Zhu JK. The unique mode of action of a divergent member of the ABA-receptor protein family in ABA and stress signaling. Cell Res. 2013; 23:1380–1395. [PubMed: 24189045]

Zhao Y, Xing L, Wang X, Hou YJ, Gao J, Wang P, Duan CG, Zhu X, Zhu JK. The ABA receptor PYL8 promotes lateral root growth by enhancing MYB77-dependent transcription of auxin-responsive genes. Sci Signal. 2014; 7:ra53. [PubMed: 24894996]

Zhao Y, Chan Z, Gao J, Xing L, Cao M, Yu C, Hu Y, You J, Shi H, Zhu Y, et al. ABA receptor PYL9 promotes drought resistance and leaf senescence. Proc Natl Acad Sci USA. 2016; 113:1949–1954. [PubMed: 26831097]

Highlights

- High-order quattuordecuple Arabidopsis PYL ABA receptor mutants were generated
- PYL-mediated signaling is critical for plant growth and development
- PYL-mediated ABA signaling antagonizes ABA-independent SnRK2 activity
- PYLs interact with and inhibit osmotic stress-activated SnRK2 protein kinases

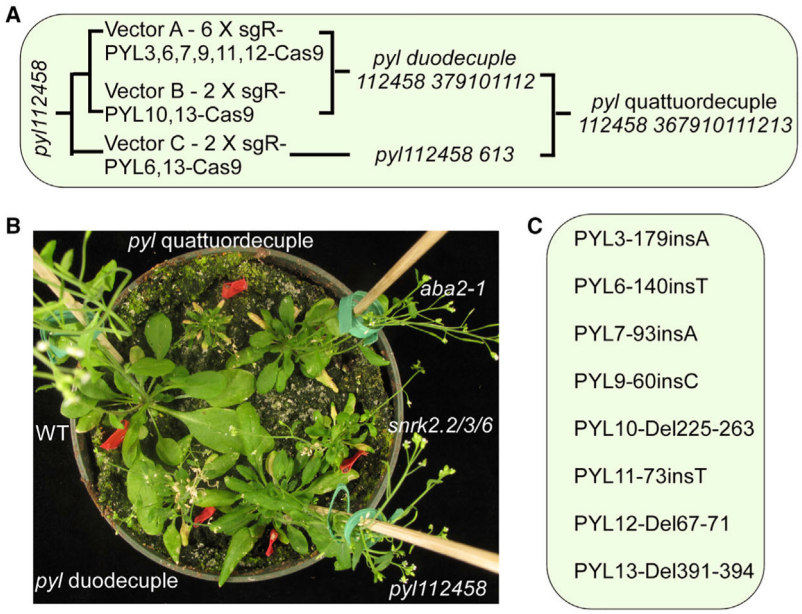

Figure 1. Generation of *pyl* Quattuordecuple Mutants

(A) Generation of *pyl* quattuordecuple mutants. To generate *pyl* duodecuple mutants, we co-transferred vector A and vector B into *112458* T-DNA sextuple mutant. To generate the *pyl112458 613* mutant, we transferred vector C into *112458* T-DNA sextuple mutant. To generate *pyl* quattuordecuple mutants, we crossed the *pyl* duodecuple mutant with the *pyl112458 613* mutant.

(B) Growth defects of the *pyl* quattuordecuple mutant.Images of representative seedlingsof the *pyl* quattuordecuple mutant, *pyl* duodecuple mutant, *pyl112458* mutant, *snrk2.2/3/6* mutant, *aba2-1* mutant, and WT. Shown are 50-day-old plants under long-day conditions grown with a plastic cover.

(C) Mutations in the *pyl* quattuordecuple mutant. Mutations in *PYL3/6/7/9/10/11/12/13* genes in the *pyl* quattuordecuple mutant. ins, insertion; Del, deletion.

See also Figure S1 and Table S1.

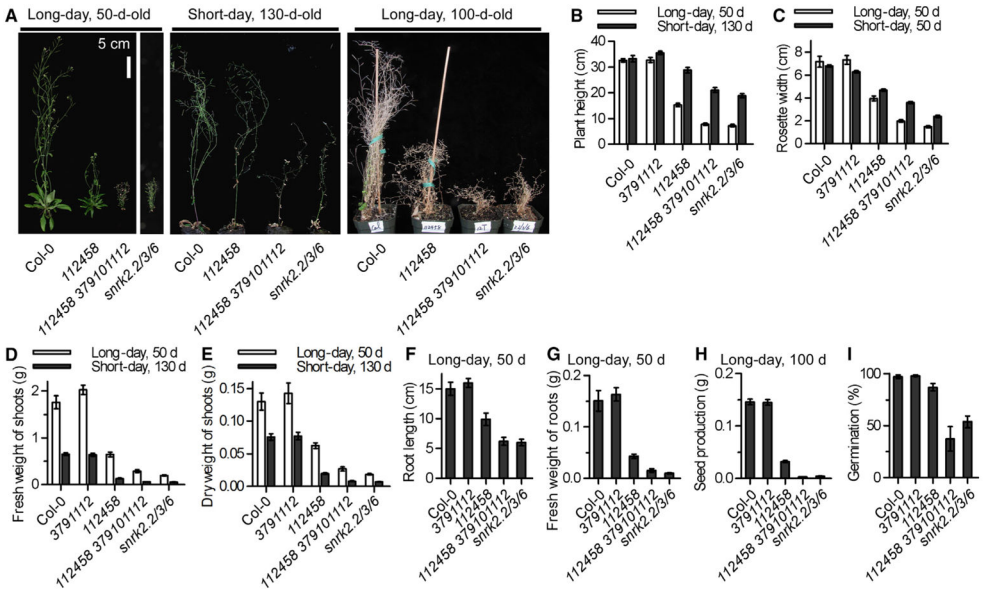

Figure 2. Growth Defects of the *112458 379101112* Mutant

(A) Images of representative seedlings of ABA-insensitive mutants in soil. Image of 50-day-old plants under long-day conditions (left panel), 130-day-old plants under short-day conditions (middle panel), and 100-day-old plants under long-day conditions with a plastic cover (right panel).

(B) Plant height of 50-day-old plants under long-day conditions and 130-day-old plants under short-day conditions. Error bars indicate SEM (n ≥ 25 seedlings).

(C) Rosette width of 50-day-old plants under long-day or short-day conditions. Error bars indicate SEM (n ≥25 seedlings).

(D and E) Fresh weight (D) and dry weight (E) of shoots of 50-day-old plants under long-day conditions and 130-day-old plants under short-day conditions. Error bars indicate SEM (n ≥15 seedlings).

(F) Root length of 50-day-old plants under long-day conditions. Error bars indicate SEM (n ≥15 seedlings).

(G) Fresh weight of roots of 50-day-old plants under long-day conditions. Error bars indicate SEM (n ≥15 seedlings).

(H) Seed production of 100-day-old plants under long-day conditions. Error bars indicate SEM (n ≥16 seedlings).

(I) Seed germination of ABA-insensitive mutants on MS plates. Error bars indicate SEM (n ≥4 different batches).

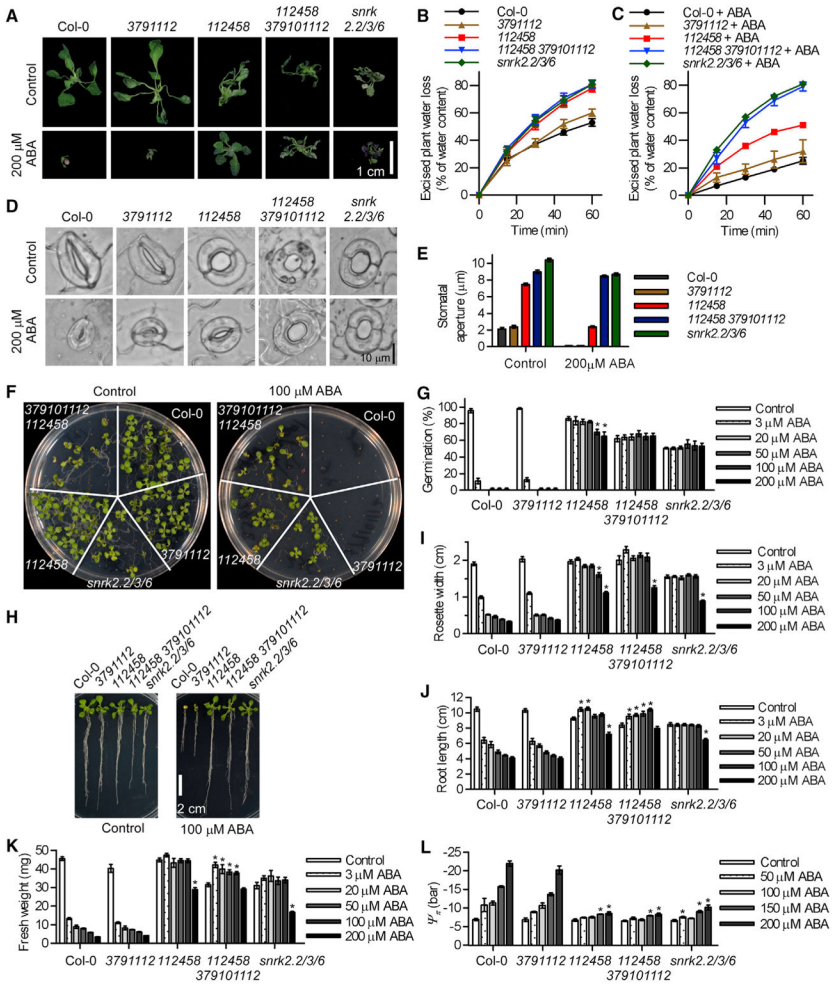

Figure 3. Extreme ABA-Insensitive Phenotypes of the *112458 379101112* Mutant

(A–C) Water loss from detached rosette of 25-day-old ABA-insensitive mutants grown on plates. Representative images show rosettes 1 hr after detached (A). Cumulative transpirational water loss from plants grown without ABA (B) or with 200 μM ABA (C). Error bars indicate SEM (n ≥ 3).

(D and E) Constitutively open stomata of the *112458 379101112* and *snrk2.2/3/6* mutants. Representative images (D) and aperture (E) of stomata in each genotype grown with or without 200 μM ABA. Error bars indicate SEM (n ≥ 90).

(F and G) Germination and growth of ABA-insensitive mutants. Representative images (F) and germination rate (G) of each genotype with or without ABA. Error bars indicate SEM (n ≥ 7). *p < 0.05, Student's t test.

(H–L) Growth of ABA-insensitive mutants were analyzed 11 days after the seedling were transferred to medium with or without ABA. Representative images (H), rosette width (I), root length (J), fresh weight (K), and osmotic potential (L) were documented. Error bars indicate SEM (n ≥ 15 seedlings) in (I–K), and SEM (n ≥ 3) in (L). *p < 0.05, Student's t test.

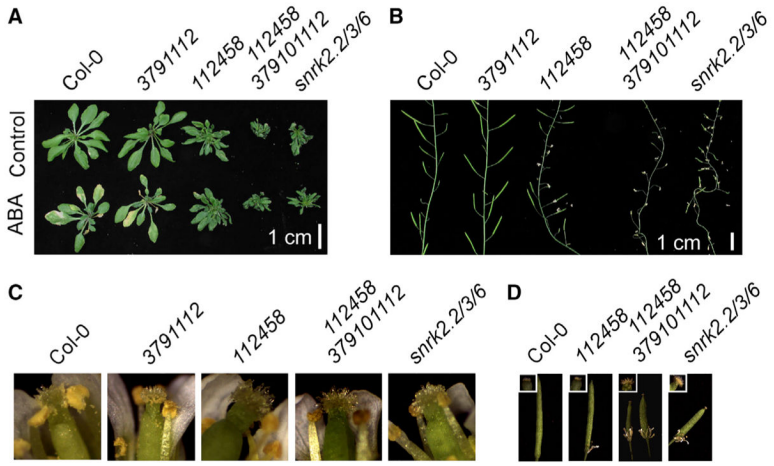

Figure 4. Senescence and Abscission Phenotypes of the *112458 379101112* Mutant

(A) ABA-induced leaf senescence in 40-day-old plants under long-day conditions.

(B) Inflorescence of 130-day-old plants under short-day conditions.

(C) Anther dehiscence in 50-day-old plants under long-day conditions.

(D) Siliques of 50-day-old plants under long-day conditions.

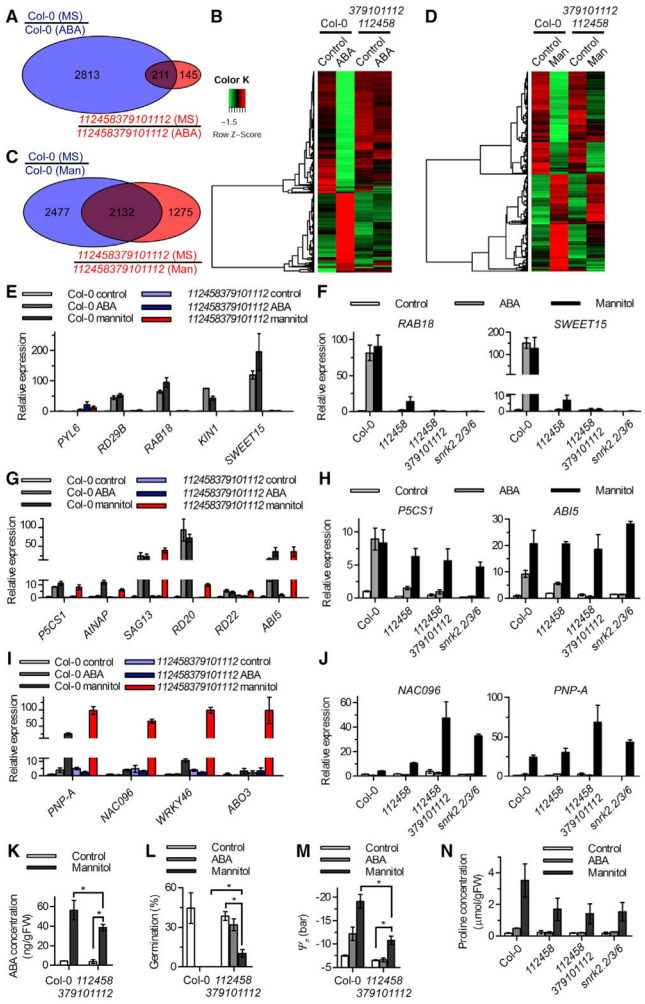

Figure 5. Gene Expression Responses to ABA and to Osmotic Stress in the *112458 379101112* Mutant

(A–D) Gene expression responses to ABA (A and B) and to osmotic stress (C and D) in the *112458 379101112* mutant. The venn diagram (A and C) and heatmap (B and D) represent genes with changed expression (2-fold or greater, false discovery rate, $p < 0.05$) in seedlings with ABA or osmotic stress treatment compared with that of control conditions.

(E–H) Relative expression of selected genes responsive to osmotic stress in an ABA-dependent manner (E and F) or ABA-independent manner (G and H). Expression of genes were assayed by quantitative RT-PCR. Error bars indicate SEM ($n \geq 3$).

(I and J) Relative expression of selected genes mainly responsive to osmotic stress but not ABA. Expression of genes were assayed by quantitative RT-PCR in *112458379101112* (I) and *snrk2.2/3/6* seedlings (J). Error bars indicate SEM ($n \geq 3$).

(K) ABA level was documented after 12 hr treatment with mannitol. Error bars indicate SD ($n = 3$)

(L) Germination was scored for radicle emergence after 24 hr with treatments of ABA and mannitol. Error bars indicate SEM ($n \geq 4$).

(M) Osmotic potential was documented after 48 hr treatment with ABA or mannitol. Error bars indicate SD ($n \geq 4$). *$p < 0.05$, Student's t test.

(N) Proline accumulation was documented after 24 hr with treatments of ABA and mannitol. Error bars indicate SD (n = 3).

See also Figures S2 and S3 and Table S2.

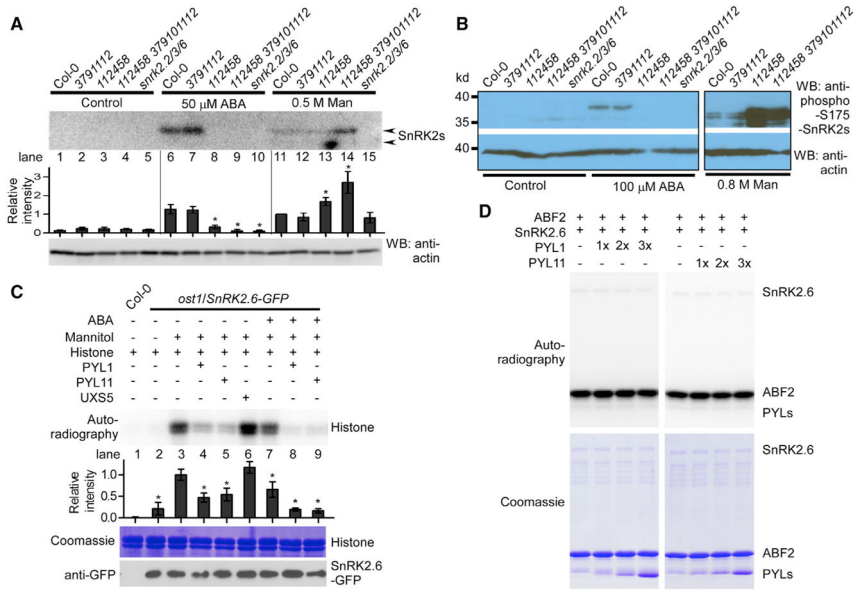

Figure 6. The Activation of SnRK2s by Osmotic Stresses Was Enhanced in *pyl* Mutants

(A) In-gel kinase assay with proteins extracted from ABA-insensitive mutants upon treatments with ABA and mannitol. Histones were used as the phosphorylation substrate. The expected position of SnRK2s was indicated by arrowheads. Radioactivity of the band was normalized with respect to the radioactivity of the band in the mannitol treated Col-0. Error bars indicate SEM ($n \geq 4$). *$p < 0.05$, Student's t test.

(B) ABA and mannitol induced auto-phosphorylation of SnRK2s in 8-day-old ABA-insensitive mutants. Anti-phospho-S175-SnRK2s antibody was used to detect auto-phosphorylation of SnRK2s. Actin was used as a loading control.

(C) Phosphorylation activity of GFP-tagged SnRK2.6 extracted from transgenic plants with mannitol treatment. SnRK2.6-GFP pre-incubated with recombinant GST-fused PYL1, PYL11, and UXS5 was incubated with histones in the presence of radioactive ATP. Phosphorylation activity of SnRK2.6-GFP was detected by autoradiography (upper panel). Radioactivity of the band was normalized with respect to the radioactivity of the band in SnRK2.6 without PYLs and UXS5 (lane 3). The input proteins of histone substrate and SnRK2.6-GFP were detected by Coomassie staining (middle panel) and western blotting with anti-GFP antibodies (lower panel). Error bars indicate SEM ($n \geq 3$). *$p < 0.05$, Student's t test.

(D) Phosphorylation activity of recombinant SnRK2.6. SnRK2.6 pre-incubated with recombinant PYL1 and PYL11 was incubated with ABF in the presence of radioactive ATP. Phosphorylation activity of SnRK2.6 was detected by autoradiography (left panel). The input proteins of ABF2 and PYLs were detected by Coomassie staining (right panel).

A TAP-IP using *ProPYL5:PYL5-HA-YFP* lines.

Symbol	Score			Coverage			Unique peptides /peptides		
	Control	ABA	Man	Control	ABA	Man	Control	ABA	Man
PYL5	114.24	76.25	78.56	58.13	58.13	54.19	7/8	6/7	5/6
PYL4/5/6							0/1	0/1	0/1
PYL9	-	-	18.45	-	-	32.09	-	-	4/5
PYL10/9	-	-		-	-		-	-	0/1
SnRK2.6	30.7	25.13	31.87	21.0	26.11	21.02	2/4	2/4	2/4
SnRK2.5/6							0/2	0/2	0/2

B TAP-IP using *ProPYL9:PYL9-HA-YFP* lines.

Symbol	Score			Coverage			Unique peptides /peptides		
	Control	ABA	Man	Control	ABA	Man	Control	ABA	Man
PYL9	193.20	173.40	207.53	81.82	81.82	85.56	12/15	11/14	12/16
PYL7/8/9/10	18.35	23.18	65.62	8.53	8.53	8.53	0/2	0/2	0/3
PYL5	-	-	18.58	-	-	15.76	-	-	3/3
SnRK2.6	75.66	42.56	69.79	26.11	26.11	26.11	2/6	2/5	2/5
SnRK2.5/6							0/2	0/2	0/2
SnRK2.2/3 /4/6/9/10							0/2	0/1	0/1
HAB2	65.21	43.63	76.34	33.07	30.92	38.75	12/13	9/10	14/16
PP2CA	22.80	55.55	49.57	24.31	49.37	47.87	5/6	11/13	10/12
ABI1	10.66	28.86	36.97	8.29	19.35	23.73	2/3	7/8	8/9
HAB1/HAB2							0/2	0/2	0/3
HAI1/PP2CA							0/1	0/2	0/2
ABI2/ABI1							0/1	0/1	0/1
HAI2/PP2CA	-			-			-	0/1	0/1
HAI3/PP2CA	-			-			-	0/1	0/1

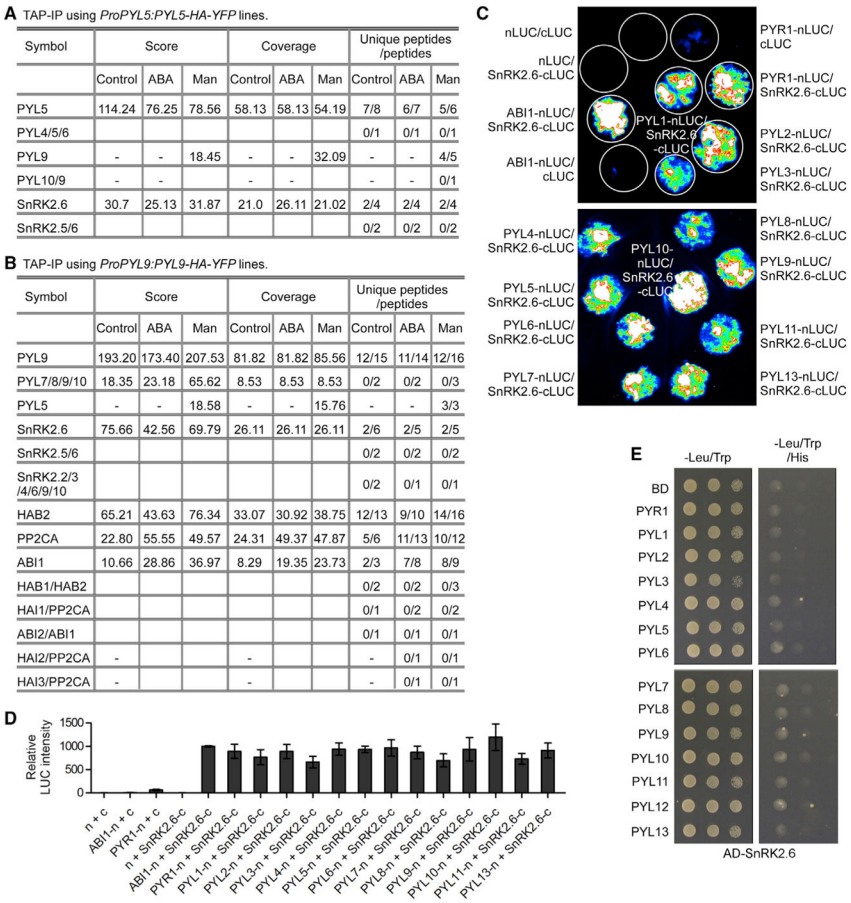

Figure 7. PYLs Interact with SnRK2s *In Vivo*

(A and B) ABA signaling core components co-immunoprecipitated with PYL5-HA-YFP (A) and PYL9-HA-YFP (B) from *ProPYLs:PYLs-HA-YFP* transgenic plants with and without mannitol or ABA treatment.

(C and D) PYLs interact with SnRK2.6 in split LUC complementation assays in *Nicotiana benthamiana* leaves. The SnRK2.6-cLUC and ABI1-nLUC combination was used as a positive control, and combinations of SnRK2.6-cLUC/nLUC and PYR1-nLUC/cLUC were used as negative controls (C). LUC signal intensity was normalized with respect to the signal intensity of the combination of cLUC/nLUC (D). Error bars indicate SD (n = 3).

(E) PYLs do not interact with SnRK2.6 in yeast two-hybrid assays. Interactions was determined by yeast growth in media lacking His with dilutions (10^{-1}, 10^{-2}, and 10^{-3}) of saturated cultures. Combination of AD-SnRK2.6 and BD was used as negative control.

See also Table S3.